

FT-IR quantification of the carbonyl functional group in aqueous-phase secondary organic aerosol from phenols



Kathryn M. George, Travis C. Ruthenburg, Jeremy Smith, Lu Yu, Qi Zhang, Cort Anastasio, Ann M. Dillner*

Crocker Nuclear Laboratory, University of California, Davis, CA 95616, USA

HIGHLIGHTS

- We employed an FT-IR technique to quantify the functional group makeup of SOA.
- We analyzed four functional groups: C=O, saturated C–H, unsaturated C–H and O–H.
- The C=O functional group accounted for up to 14% of the phenolic SOA sample mass.
- Acids measured by ion chromatography account for ~20% of carbonyl reported by FT-IR.

ARTICLE INFO

Article history:

Received 21 June 2014

Received in revised form

31 October 2014

Accepted 5 November 2014

Available online 6 November 2014

Keywords:

SOA

Fourier transform infrared spectroscopy

Phenol

Carboxylic acids

ABSTRACT

Recent findings suggest that secondary organic aerosols (SOA) formed from aqueous-phase reactions of some organic species, including phenols, contribute significantly to particulate mass in the atmosphere. In this study, we employ a Fourier transform infrared (FT-IR) spectroscopic technique to identify and quantify the functional group makeup of phenolic SOA. Solutions containing an oxidant (hydroxyl radical or 3,4-dimethoxybenzaldehyde) and either one phenol (phenol, guaiacol, or syringol) or a mixture of phenols mimicking softwood or hardwood emissions were illuminated to make SOA, atomized, and collected on a filter. We produced laboratory standards of relevant organic compounds in order to develop calibrations for four functional groups: carbonyls (C=O), saturated C–H, unsaturated C–H and O–H. We analyzed the SOA samples with transmission FT-IR to identify and determine the amounts of the four functional groups. The carbonyl functional group accounts for 3–12% of the SOA sample mass in single phenolic SOA samples and 9–14% of the SOA sample mass in mixture samples. No carbonyl functional groups are present in the initial reactants. Varying amounts of each of the other functional groups are observed. Comparing carbonyls measured by FT-IR (which could include aldehydes, ketones, esters, and carboxylic acids) with eight small carboxylic acids measured by ion chromatography indicates that the acids only account for an average of 20% of the total carbonyl reported by FT-IR.

© 2014 Elsevier Ltd. All rights reserved.

1. Introduction

On global and regional scales, organic aerosols (OA) are a dominant fraction of atmospheric particulate matter (Heald et al., 2010). While a significant portion of OA is secondary in nature, large discrepancies exist between modeled atmospheric secondary organic aerosol (SOA) concentrations and observations from field and laboratory studies (Hallquist et al., 2009). Traditional models generally focus on SOA formation from the gas-phase oxidation of volatile

organic compounds to produce low-volatility SOA (e.g. Donahue et al., 2012). However, the magnitude of SOA production from reactions in the gas-phase fails to predict ambient SOA loadings and variability (Rudich et al., 2007). Understanding characteristics of SOA produced from reactions taking place in the aqueous phase may aid in remedying model discrepancies and uncovering impacts on climate forcing and human health (Ervens et al., 2011).

Phenols are one family of aromatic compounds that produce SOA via gas-phase reactions (Yee et al., 2013; Nakao et al., 2011) and are also water-soluble and participate in the aqueous-phase formation of SOA (Smith et al., 2014; Chang and Thompson, 2010). A number of different groups of phenols are emitted from biomass combustion (Hawthorne et al., 1989; Schauer et al., 2001). Three of the major groups include those based on the structures of phenol

* Corresponding author. Crocker Nuclear Laboratory, 1 Shields Ave., University of California, Davis, CA 95616, USA.

E-mail address: amdillner@ucdavis.edu (A.M. Dillner).

(PhOH, i.e., C₆H₆OH), guaiacol (GUA, 2-methoxyphenol), and syringol (2,6-dimethoxyphenol): the emitted compounds within each of these groups include the base structure (e.g., GUA) as well as many different substituted compounds built from that base (e.g., methyl-substituted guaiacol). Emission rates for phenols from wood combustion range from 400 to 900 mg kg⁻¹ fuel and vary based on the type of wood burned (Hawthorne et al., 1989; Schauer et al., 2001). Though primarily emitted as gases, phenols readily partition to the aqueous-phase with Henry's law constants up to 10⁶ M atm⁻¹ (Sander, 1999). Once in the aqueous-phase, phenols are highly reactive with common atmospheric oxidants such as hydroxyl radical and excited triplet states of aromatic carbonyl compounds, resulting in phenol lifetimes of less than a day (Smith et al., 2014; Sun et al., 2010).

Recently, studies on aqueous-phase photochemical reactions involving phenols have shown the formation of low volatility, high-molecular weight products with oxygen-to-carbon ratios similar to those of ambient low-volatility oxygenated organic aerosol (Yu et al., 2014; Sun et al., 2010). These studies employ techniques such as mass spectroscopy and ion chromatography to characterize the SOA mass. While these techniques are information-rich in terms of organic composition, a technique with specificity in regards to functional group composition would assist in establishing a more complete picture of the chemical makeup of aqueous-phase reaction products.

Fourier transform infrared spectroscopy (FT-IR) is a useful tool for identifying and quantifying the functional group composition. A functional group absorbs radiation at a characteristic frequency (Smith, 1998). The magnitude of this absorbance, which is proportional to the moles of the functional group, is used in quantifying the amount of a functional group in a particular sample. Though distinguishing between specific bond configurations (e.g., ketone vs. carboxylic acid C=O) can be difficult, an infrared spectrum can be readily utilized to identify and quantify functional groups within a mixture.

Previous studies have applied FT-IR to characterize and sometimes quantify organic functional groups in ambient aerosol samples (Ruthenburg et al., 2013; Russell et al., 2011) and from laboratory studies (Najera et al., 2009) including those evaluating SOA (Ofner et al., 2010; Chang and Thompson, 2010). Functional groups including O–H, C–H, and C=O have been quantified using FT-IR analysis for ambient samples in many environments including pristine (Ruthenburg et al., 2013), marine (Russell et al., 2011), fire impacted (Takahama et al., 2011), and urban (Takahama et al., 2013b; Polidori et al., 2008). Studies in the laboratory have evaluated the time-resolved evolution of functional groups during the aerosol formation process (Ofner et al., 2011) and identified structural components for source apportionment purposes (Chang and Thompson, 2010).

Both univariate (Russell et al., 2009; Takahama et al., 2013a) and multivariate (Coury and Dillner, 2008; Ruthenburg et al., 2013) regression techniques have been utilized to quantify functional groups. Univariate methods typically use extensive spectral manipulation techniques, such as background correction, baseline-correction algorithms and peak fitting, in order to resolve functional group mass in samples (Takahama et al., 2013a). Partial least squares regression (PLS), a multivariate method, has been used to correlate absorbance with known moles of functional groups (Ruthenburg et al., 2013; Coury and Dillner, 2008). While no spectral manipulation is needed for PLS, it is dependent on calibration standards that mimic the samples and uses complex statistics to create calibration models.

For this study, we developed a univariate spectral analysis method to quantify the functional groups in laboratory-generated aqueous-phase SOA from phenols. We utilized FT-IR spectroscopy

to resolve organic functional groups in the complex, highly aromatic, SOA samples. Calibration standards were prepared from atmospherically relevant compounds containing one or more of the functional groups: O–H, saturated C–H, unsaturated C–H and C=O. We integrated peaks and used a straightforward linear regression technique to determine the amount of functional groups in order to characterize the makeup of our phenolic SOA samples. This simplified approach was utilized to decrease spectral manipulation relative to peak fitting techniques and improve interpretability compared to statistical techniques. Our method was developed specifically for the chemical composition found in the laboratory samples generated for this work. Although we present the results for all four functional groups listed above to fully characterize the SOA, we focus our investigation on carbonyls. We first present a qualitative evaluation of the FT-IR spectra. This is followed by quantification of the carbonyl group in all samples and comparing this to measurements of small carbonyl-containing acids from ion chromatography. We then discuss the quantification of the three other functional groups and apply all of the calibrations to samples that mimic hardwood and softwood samples.

2. Experimental setup and methods

2.1. SOA generation

We produced aqueous-phase SOA by reacting three phenols (phenol, guaiacol, and/or syringol) with either •OH (formed from the photolysis of hydrogen peroxide) or the triplet excited state of 3,4-dimethoxybenzaldehyde (DMB) in bulk solutions. Solutions were prepared with air-saturated, purified water from a Milli-Q system. All chemicals were used as received: phenol (PhOH; 99%), 3,4-dimethoxybenzaldehyde (DMB; 99%), syringol (SYR; 99%), and guaiacol (GUA; 98%) from TCI America; hydrogen peroxide (30%) was from Fisher. For solutions containing a single phenol, we used a phenol concentration of 100 μM and added an oxidant precursor (either 100 μM hydrogen peroxide or 5 μM DMB) and 5 μM H₂SO₄ to make solutions to pH 5 (Smith et al., 2014). We also examined the DMB-mediated reactions of mixtures of phenols that mimic emissions from hardwood and softwood burning. Hardwood solutions contained 33 μM phenol, 7 μM guaiacol, and 60 μM syringol; softwood solutions contained 79 μM phenol and 21 μM guaiacol. The initial total concentration of 100 μM phenol is approximately what is expected in atmospheric waters in regions with significant wood combustion (Anastasio et al., 1997; Schauer et al., 2001).

Solutions were illuminated in air tight, stirred, Pyrex tubes in a Rayonet photoreactor system (model RPR-200) equipped with three different types of bulbs to roughly mimic sunlight. As described in Supplemental material section S1, oxidant levels in solutions illuminated in the RPR-200 are approximately 7 times higher than in ambient, wintertime fog drops, both for •OH and for the triplet excited state of DMB. In each illumination experiment a dark control sample was wrapped in aluminum foil, placed in the photoreactor and treated identically to the illuminated cell. For solutions containing one phenol, we illuminated the solution until half of the phenol had decayed, as monitored by HPLC with UV–Vis detection (Smith et al., 2014; Supplemental section S1). For phenol mixtures we illuminated until half of the total initial phenol concentration was lost. Illumination times ranged from approximately 1 h for syringol to 10 h for phenol (Table S1 in supplemental material).

Upon reaction completion, 10 or 12 mL of the illuminated and control solutions were placed in separate aluminum cups and blown to dryness with N₂ at room temperature (Smith et al., 2014). Cups were weighed before and after adding the sample to determine the gravimetric mass of the low volatility material formed

during illumination. The dark control mass was subtracted from the illuminated sample mass, with the difference representing the mass of low volatility SOA (Smith et al., 2014). The remaining aqueous material was flash-frozen in liquid nitrogen in a Teflon bottle for FT-IR sample preparation and analysis.

2.2. Filter collection for FT-IR analysis

Flash-frozen SOA solutions were stored in a freezer at $-20\text{ }^{\circ}\text{C}$ and removed to thaw in the laboratory immediately prior to use. Aqueous-phase samples were atomized using a constant output aerosol generator (Model 3076, TSI Inc., St. Paul, MN). The atomizer was supplied with house compressed air that was purified and dried (Model 3074B Filtered Air Supply, TSI Inc., St. Paul, MN). A water trap and diffusion dryer filled with silica desiccant were located before the filter assembly to remove water from the particles. Particles were collected on 25-mm polytetrafluoroethylene (PTFE) filters (25 mm diameter 0.3 μm pore size[®], Pall Corporation, Port Washington, NY) in an assembly that was constructed using Interagency Monitoring of Protected Visual Environments (IMPROVE) network (<http://vista.cira.colostate.edu/improve/>) PTFE PM_{2.5} cassettes (McDade et al., 2009). PTFE filters were analyzed by FT-IR before and after sample collection and pre- and post-weighed (in triplicate) on an ultra-microbalance (XP2U, Mettler Toledo, Columbus, OH) with 0.2 μg repeatability. Sample mass was determined by the difference of pre- and post-averages. For all gravimetric measurements, mass uncertainty was calculated using the root mean square (RMS) of the standard deviation of the pre- and post-measurements. Gravimetric measurements for all samples had RMS errors of 2 μg or less.

Each dark control sample was atomized directly before its corresponding illuminated SOA sample. Milli-Q blanks were run between light/dark pairs. In the case of single phenol samples, we atomized and collected a replicate filter using an SOA sample generated on a different day. Two or three filters from each hardwood and softwood solution were collected. We calculated the SOA mass by subtracting the sulfate mass (calculated from sulfuric acid concentration added to the sample) from the total filter mass. In order to determine if phenols or oxidants were collected on filters, solutions of each precursor were atomized, dried and collected on filters. The resulting gravimetric and FT-IR measurements showed no evidence of precursors. We are therefore confident that all remaining precursors in SOA solutions evaporated during atomization and were not collected on the sample filters.

2.3. FT-IR analysis

A Bruker Tensor 27 FT-IR (Bruker Optics, Billerica, MA) equipped with a liquid nitrogen-cooled mercury cadmium telluride detector was operated with OPUS spectroscopy software to obtain infrared spectra. The spectrometer was purged with clean, dry air provided by a PureGas purge gas generator and an oil-less air compressor to minimize water and CO₂ absorbances in the collected spectrum.

The sample chamber was purged for 240 s before obtaining a reference or sample spectrum. Spectra were obtained in transmission mode between 4000 cm^{-1} and 420 cm^{-1} with a 4 cm^{-1} resolution by averaging 512 scans. Absorbance spectra were calculated using a spectrum of the sample chamber with no filter as the reference spectrum.

2.4. Calibrating the FT-IR method

Calibration standards for four functional groups (C=O, saturated C–H, unsaturated C–H, O–H) were prepared by atomizing low concentration aqueous or ethanolic solutions of individual organic compounds (Sigma–Aldrich, St. Louis, MO) and collecting the particles on PTFE filters, using a similar setup as used for collecting SOA samples (Section 2.2). Collection times varied in order to produce standards with a range of masses relevant to the SOA samples.

Six compounds are used to develop a calibration for carbonyl (Table 1). The number of moles of carbonyl on each calibration standard was determined from the gravimetric mass of the collected compound, the known molecular weight of the compound and the number of carbonyl groups per molecule for the compound. The number of moles was then divided by the filter area to obtain the $\mu\text{moles}/\text{cm}^2$ of C=O on a standard. The carbonyl masses on each filter ranged from non-detectable to 30 μg .

The first step in the development of a calibration curve is determining the wavenumber region in which C=O absorbs. We evaluated standard spectra in order to define characteristic absorption wavenumbers for the C=O functional group (Fig. 1). We then calculated the area of the C=O peaks by two-point baseline correcting and integrating within the listed integration regions (Table 1) using a script written in the Python programming language. Spectral integration and baseline regions differed slightly between compounds to include relevant spectral features but exclude noise or interferences such as PTFE peaks. Peaks in the C=O absorbances ranged from 1750 to 1660 cm^{-1} for all of the standards. The ester (arachidyl dodecanoate) absorbed at the highest wavenumbers in the carbonyl region, with a peak center located at 1735 cm^{-1} , while ketone and carboxylic acid C=O peaks were centered 1700 cm^{-1} . The peak in benzoic acid was present at a lower wavenumber, 1680 cm^{-1} , likely because of the aromaticity of the compound.

A C=O calibration curve was obtained by regressing the integrated absorbance ($\text{a.u.}\cdot\text{cm}^{-1}$) and measured moles of bonds per filter deposition area ($\mu\text{mol}/\text{cm}^2$). Six blank filters were also baseline corrected, integrated and included in each compound calibration curve; since the blank absorbances were negligible the linear regression was forced through the origin. Absorptivities for each standard compound (Table 1) were calculated from each standard's regression slope. The absorptivities are consistent even between differing carbonyl-containing compounds (i.e. ketone and carboxylic acid) for all standards evaluated for the C=O region. Therefore, standards were regressed together to obtain one calibration curve, with an absorptivity of $11.38\text{ a.u.}\cdot\text{cm}^{-1}/\mu\text{mol}\cdot\text{cm}^{-2}$ and a 95%

Table 1
Compounds used for FT-IR C=O calibration. Peak integration regions are reported, along with the number of standards used in the calibration (*n*) and the calculated molar absorptivities (reported in $\text{a.u.}\cdot\text{cm}^{-1}/\mu\text{mol}\cdot\text{cm}^{-2}$ of carbonyl).

Compound name	Compound class	Chemical formula	<i>n</i>	Integration region (cm^{-1})	Absorptivity \pm std deviation ($\text{a.u.}\cdot\text{cm}^{-1}/\mu\text{mol}\cdot\text{cm}^{-2}$)
12-Tricosanone	Ketone	C ₂₃ H ₄₆ O	16	1768–1660	12.0 \pm 0.4
Succinic acid	Dicarboxylic acid	C ₄ H ₆ O ₄	10	1755–1665	11.9 \pm 0.6
Adipic acid	Dicarboxylic acid	C ₄ H ₁₀ O ₄	18	1755–1666	12.3 \pm 1.8
Suberic acid	Dicarboxylic acid	C ₈ H ₁₄ O ₄	24	1755–1665	11.6 \pm 0.6
Benzoic acid	Aromatic carb. acid	C ₇ H ₆ O ₂	10	1741–1664	13.0 \pm 1.2
Arachidyl dodecanoate	Ester	C ₃₂ H ₆₄ O ₂	27	1760–1690	9.9 \pm 1.8

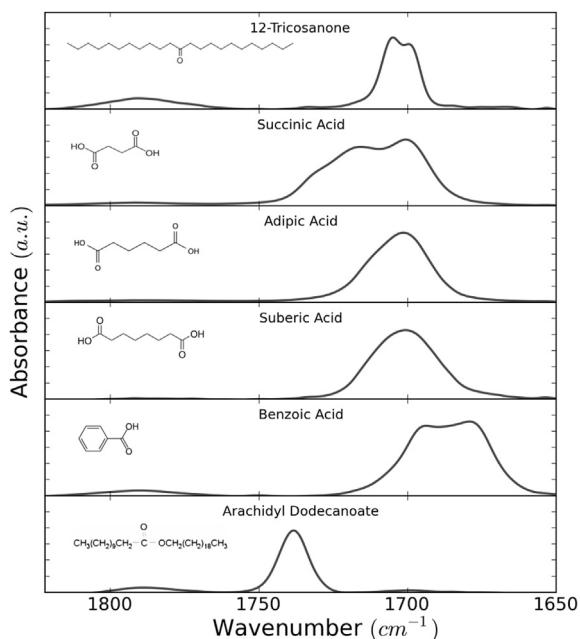


Fig. 1. FT-IR spectra of compounds used in C=O calibration. Spectra have been scaled to view absorbance features and the chemical structures are displayed.

confidence interval error of $0.23 \text{ a.u.} \cdot \text{cm}^{-1} / \mu\text{mol} \cdot \text{cm}^{-2}$ (Fig. 2). Our values are comparable to the $11.2 \pm 1.7 \text{ cm}^{-1} \mu\text{mol}^{-1}$ carbonyl group absorptivity for aerosols collected on Teflon filters reported by Takahama et al. (2013a).

Calibrations for saturated C–H, unsaturated C–H, and O–H bonds were also developed to semi-quantitatively evaluate these groups in the SOA samples (Section S2 in supplemental material).

2.5. Spectral analysis parameters for SOA samples

Characteristic absorbance regions for the different functional groups in the SOA spectra were chosen using calibration data and

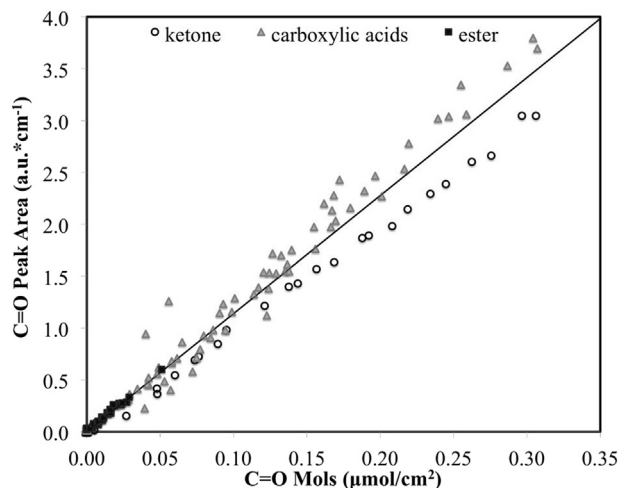


Fig. 2. C=O calibration curve (bond peak area vs. bond moles/filter deposition area) for all carbonyl-containing compounds. Carbonyl compounds are identified in the figure by their class of compound (ketone, carboxylic acids and ester) as listed in Table 1. Spectra of these compounds are shown in Fig. 1. The line indicates the regression fit for all carbonyl standards ($m = 11.38$, $r^2 = 0.97$).

previously published literature (Fig. 1; Coates, 2000; Smith, 1998). Different wavenumbers were used as limits for baseline correction and integration in the O–H region in order to baseline at wavenumbers closest to zero absorbance in the SOA spectra. In the SOA samples, we used absorbances in the following wavenumber ranges for each functional group: carbonyl, $1830\text{--}1660 \text{ cm}^{-1}$; O–H, $3670\text{--}2640 \text{ cm}^{-1}$; saturated C–H, absorbance atop the O–H peak below 3000 cm^{-1} ; and unsaturated C–H, $3100\text{--}3000 \text{ cm}^{-1}$. Peaks at wavenumbers corresponding to the C–F bonds present in PTFE filters ($1288\text{--}1020 \text{ cm}^{-1}$) and below were excluded from any form of analysis in this study. To obtain the moles (and mass) of carbonyl and other functional groups in the SOA samples the calibration was applied to the integrated areas. The percentage of each functional group (functional group mass divided by SOA mass on the filter) was calculated as a metric for comparing samples.

2.6. Detection limits and measurement precision of the carbonyl functional group in SOA

Method detection limits (MDLs) were calculated using FT-IR spectra of 25 blank filters. These filters were subsequently used to collect SOA or Milli-Q blank samples. Spectra were baseline corrected and integrated, applying the same integration regions and procedure used for standard and sample spectra. The mass of functional groups on each blank filter was obtained using the calibration curves (Fig. 2 and S1). The MDL for each functional group, as shown in Table 2, is defined as 3 times the standard deviation of the functional group masses determined on the blanks. The large MDL determined for the O–H functional group evidences the non-linearity in the PTFE spectrum in this region.

Spectral precision was calculated using five scans from one blank filter. A reference spectrum was first obtained; then, the filter was placed in the sample chamber, scanned, and removed from the instrument. This process was repeated over a period of three days to obtain five spectra, which were then converted to functional group mass (Section 2.5). The precision is calculated as the standard deviation of these masses multiplied by three. As with MDL and blank levels, precision was the best in the carbonyl region and worst in the O–H region (Table 2). This precision calculation takes into account the variability due to instrumental drift, background conditions, and sample alignment.

Calibration uncertainty (Table 2) was determined for each functional group. These uncertainties, calculated using the relative standard deviation of the absorptivities of the different standard compounds for a given functional group (provided in Table 1) are larger than those based on the blank spectra and are used for reporting measurement uncertainty. The calibration uncertainties for C=O and C–H were less than 10% with significantly greater uncertainties for O–H and unsaturated C–H.

2.7. Additional instrumentation

Organic anions in the SOA samples were analyzed with a Metrom ion chromatography (IC) system (Yu et al., 2014). Eight

Table 2
Detection limits, spectral precision, and calibration uncertainty for each evaluated functional group.

Functional group	MDL ($\mu\text{mol}/\text{cm}^2$)	Spectral precision ($\mu\text{mol}/\text{cm}^2$)	Calibration uncertainty (%)
C=O	2.7E-03	4.0E-04	8.9
Saturated C–H	6.8E-02	9.7E-03	5.1
Unsaturated C–H	7.1E-03	4.0E-02	25.3
O–H	2.0E-01	4.1E-02	40.9

organic ions (malate, fumarate, malonate, oxalate, maleate, pyruvate, formate, and glyoxylate) that contain the carbonyl functional group were measured in the SOA samples. Ions were measured in SOA sample solutions that had been blown to dryness with N_2 (Smith et al., 2014) and reconstituted using Milli-Q water (i.e., “blowdown” samples). Masses of organic acids present on SOA filters were determined using measured acid concentration ($\mu\text{g}/\text{mL}$), solution atomization volume (mL) and collection efficiency (%). Blowdown IC $\text{C}=\text{O}$ is directly relatable to FT-IR $\text{C}=\text{O}$ because the atomization and drying technique used for FT-IR, and the blowdown technique for the IC samples, both remove high volatility and semi-volatile species present in the SOA.

3. Results

3.1. SOA spectral analysis

Qualitative analysis of spectra of aqueous-phase phenolic SOA reveals the presence of strong absorbance bands associated with the $\text{C}=\text{O}$ functional group in every sample (Fig. 3). Since the phenol precursors and SOA dark controls (Fig. S5) do not contain these oxygenated functional groups, the carbonyl groups were formed by aqueous-phase photochemical reactions. This is consistent with aerosol mass spectrometry analyses, which have found that the phenolic SOA from both gas and aqueous reactions contains carbonyl functional groups (Yee et al., 2013; Sun et al., 2010) and previous qualitative FT-IR work (Ofner et al., 2010; Chang and Thompson, 2010). Work conducted by Yu et al. (2014) details mechanisms for the formation of functionalized monomer and oligomer species with varying degrees of $\text{C}=\text{O}$ functionality from aqueous-phase phenolic reactions. They also suggest the formation of carbonyl-containing ring-opening species from these reactions.

As shown in Fig. 3, there are small variations in the location of the absorption peaks between the various phenols and oxidants. This is probably a result of molecular spatial and structural factors, such as substitution and conjugation patterns. The SOA spectra

contain many broad peaks, and fewer sharp peak features compared to single-component calibration standards, indicating that the SOA is composed of a mixture of many compounds. Syringol SOA contains fine structure peaks in the carbonyl region that can be resolved into two main absorptions peaking at 1735 cm^{-1} and 1696 cm^{-1} . Guaiacol and phenol SOA have broader absorbance bands in the carbonyl region, with phenol SOA exhibiting the lowest intensity absorbance in this region. Hardwood and softwood SOA mixtures contain broader $\text{C}=\text{O}$ absorbances that most closely resemble absorbances in guaiacol SOA (Fig. 3). This is potentially due to the combination of starting phenolic compounds in the hardwood and softwood SOA samples (with guaiacol present in both cases) producing compounds containing a broad range of carbonyl classes.

The carbonyl stretching vibrations are attributed to several different carbonyl-containing functional groups. Absorbance bands located from 1730 to 1700 cm^{-1} are indicative of carboxylic acids and ketones (Fig. 1 and Coates, 2000). The sharp peak at 1696 cm^{-1} suggests significant amounts of these compounds in the syringol SOA. Phenol SOA also appears to contain carboxylic acids that are likely aromatic in nature, as the $\text{C}=\text{O}$ peak is shifted to lower wavenumbers (Ofner et al., 2010; Fig. 1, benzoic acid). Bands in the carbonyl region at frequencies above 1730 cm^{-1} indicate the presence of esters (Fig. 1, arachidyl dodecanoate), suggesting that the syringol, guaiacol SOA, hardwood and softwood SOA samples also contain some esters. However, broad, overlapping peaks in the hardwood, softwood, guaiacol and phenol SOA make differentiation between specific types of carbonyl difficult and indicate the presence of a broad range of carbonyl-containing compounds.

The aromatic structure of SOA from phenolic precursors is observed in the spectra by the $\text{C}=\text{C}$ ring-related stretching vibrations between 1650 and 1580 cm^{-1} (Coates, 2000). This is readily distinguishable in spectra of syringol SOA and phenol SOA (from OH oxidation) by the well-defined peak at approximately 1600 cm^{-1} (Fig. 3). Guaiacol and phenol SOA (from DMB oxidation) display a broader peak centered at the same wavenumber. All

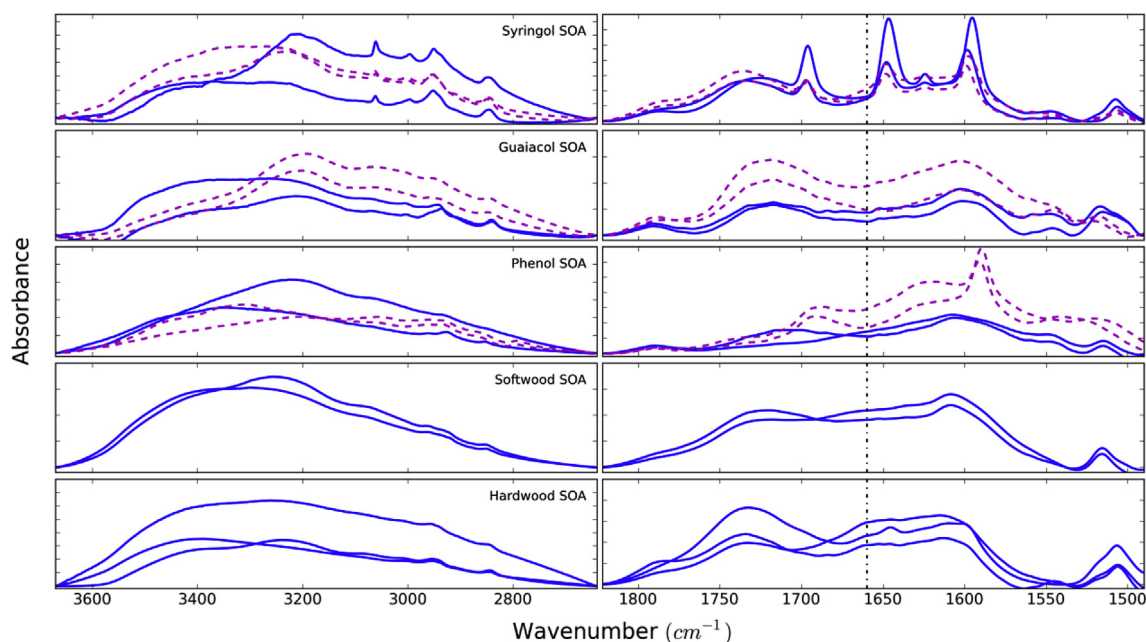


Fig. 3. FT-IR spectra of the $\text{C}=\text{O}$ region (right panel) and $\text{O}-\text{H}$ and $\text{C}-\text{H}$ (left panel) of illuminated SOA samples from the three individual phenols, softwood mixture and hardwood mixture SOA. Each spectrum within a panel represents an individual filter. Magenta spectra with dashed lines are samples that were oxidized by OH, blue spectra with solid lines were oxidized by DMB. Spectra have been mass normalized by dividing the absorbance of each spectrum by the SOA sample mass. The lower wavenumber limit of the carbonyl region is defined by the dashed vertical line at 1660 cm^{-1} . (For interpretation of the references to color in this figure legend, the reader is referred to the web version of this article.)

spectra also exhibit absorption bands in the unsaturated C–H region (3100–3000 cm^{-1}), suggesting aromaticity (Fig. 3). However, the peak shape of the unsaturated C–H region is different for each phenolic, likely due to the nature and number of substituents on the rings. This is exemplified by the sharp peak at 3065 cm^{-1} in syringol SOA versus broader, small peaks above 3000 cm^{-1} in guaiacol, phenol and mixture SOA. The presence of C=C and unsaturated C–H absorbances indicates that many of these SOA products are aromatic, as expected from monomer, dimer, and higher oligomer products of phenolic reactions (Yu et al., 2014).

Saturated C–H absorbances, assigned to the C–H stretching of methyl and methylene groups of aliphatic chains, are also present in the spectra of all SOA samples. Their presence is indicated by the relatively sharp peaks located below 3000 cm^{-1} that lie atop the O–H absorbance (Fig. 3). This suggests that some functionality is aliphatic in nature, either from individual aliphatic compounds formed by ring-opening processes or from aliphatic groups attached to aromatic rings (Yu et al., 2014).

A broad absorbance feature between 3670 and 2640 cm^{-1} (the limits of the left-hand plots in Fig. 3) in all SOA samples defines the O–H region. The O–H peak, which has the broadest functional group absorption, is attributed to phenol, hydroxyl, and carboxylic acid O–H stretching vibrations. O–H is present in our SOA spectra as expected from the hydroxylated products shown in Yu et al. (2014) formed by the addition of $\cdot\text{OH}$ to the aromatic ring. The peak shapes for different phenolic SOA samples and the hardwood and softwood mixtures are very similar in this region (Fig. 5).

Fig. 3 shows that SOA spectra from the same precursor phenol look more similar than the spectra of SOA from the same oxidant (but different phenols), indicating that the precursor phenol has a greater influence on product composition than the oxidant. Though the general spectral shapes are similar, spectra of the same starting phenol and oxidant differ in absorption intensity between samples, even when normalized by mass. This suggests that small differences in SOA preparation or atomization might alter the SOA composition on the filter. Overall, while products within a phenolic group might have very similar structures, the relative amounts of the functional groups can be different.

We have also examined spectra of the material collected from atomized dark control solutions. As displayed in Fig. S5 in the supplemental material, the dark controls for syringol samples absorb very little in the carbonyl region compared to the

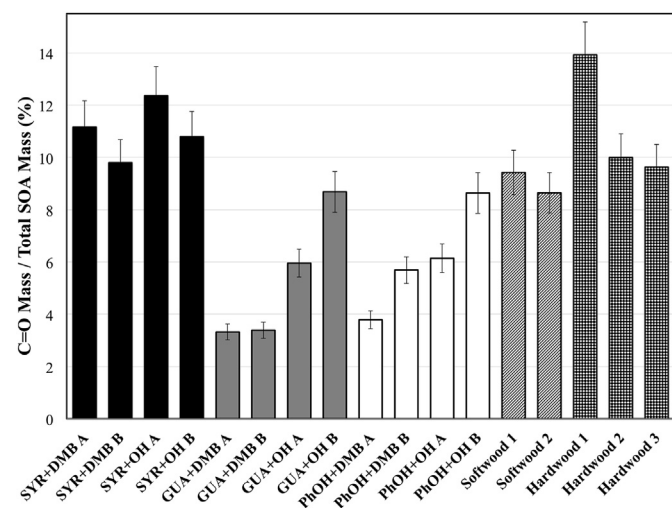


Fig. 4. Contributions of C=O to total SOA mass. A and B (and 1, 2, and 3) represent replicate SOA experiments for the same condition. Error bars represent measurement uncertainty.

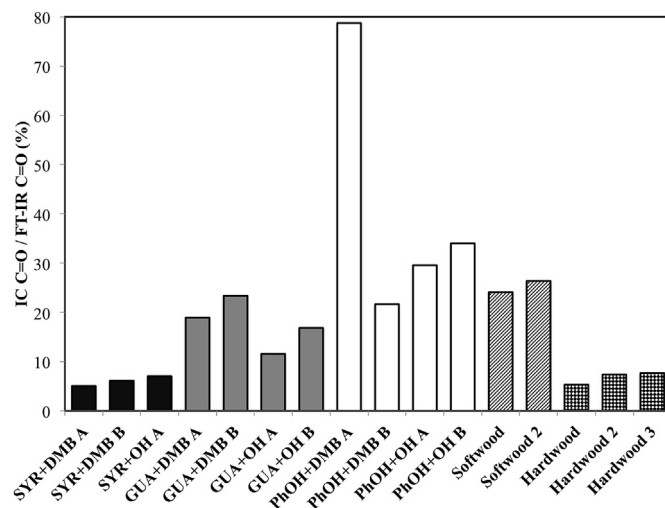


Fig. 5. Ratio of C=O in 8 organic acids measured by IC and total carbonyl measured by FT-IR. IC data is not available for the sample SYR + OH B.

illuminated samples; this is the case for all starting phenolic (including mixtures) and oxidant samples. Dark control samples do, however, absorb in the O–H region (Fig. S5). In the case of syringol SOA, the dark controls display O–H absorbances very similar to the light SOA samples; the same situation occurs for dark controls for the other phenolic SOA samples. This O–H absorbance does not appear to be from N–H (e.g., due to ammonium), as the peak shape does not resemble ammonium sulfate reference spectra. However, dark O–H absorption may be influenced by natural PTFE variability and instrumental insensitivity in the region. Dark controls for all phenolics also exhibit a small amount of saturated C–H stretching but minimal unsaturated C–H (Fig. S5). Due to the significant O–H absorbances present in dark samples, we focus on quantifying C=O and C–H in our SOA samples.

3.2. Quantification of carbonyls

Masses of C=O were determined using the suite of calibration standards (Table 1 and Fig. 1) and are listed in Table S3 in the supplemental material. In all SOA samples the carbonyl mass is significantly above the method detection limit. Fig. 4 shows the measured sample functional group masses normalized by SOA sample mass. Of the SOA samples made from individual phenols, syringol SOA contained the greatest percentage of carbonyl, with $11 \pm 1\%$ of the SOA mass attributed to C=O bonds. Guaiacol and phenol SOA samples had approximately half as much carbonyl as syringol SOA, $5 \pm 3\%$ and $6 \pm 2\%$ respectively. The SOA formed from the hardwood mixture of phenols was the most similar to syringol SOA, with a C=O percentage of $11 \pm 2\%$. C=O accounted for $9.0 \pm 0.6\%$ of the total SOA mass generated from softwood mixture phenols. SOA formed from the reactions of guaiacol and phenol had greater amounts of carbonyl with OH as the oxidant compared to with DMB. Carbonyl functional groups represent between 3 and 14% of phenolic SOA mass in these samples.

3.3. Comparison of FT-IR carbonyl with IC carboxylic acids

The carbonyl masses from the organic acids quantified by IC (as described in Section 2.7) are compared to the carbonyl masses determined by FT-IR. As shown in Fig. 5, the C=O mass determined by FT-IR is 1–20 times greater than the combined C=O mass in the 8 organic acids determined by IC. This indicates that small carboxylic acids represent a small portion of the SOA carbonyls. For

syringol SOA, small carboxylic acids account for 5–7% of C=O measured by FT-IR. In contrast, in the phenol SOA, small carboxylic acids account for 22–79% of C=O determined by FT-IR. The small carboxylic acids typically account for the least amount of FT-IR carbonyl in SOA made from syringol and the hardwood mixture (60% syringol + 33% phenol + 7% guaiacol) and the greatest amount in phenol SOA. SOA made from the softwood mixture (79% phenol and 21% guaiacol) has a percentage of carbonyls that is similar to SOA from both guaiacol and phenol with DMB. Over 90% of the carbonyls in syringol and hardwood SOA are compounds not measured by IC, i.e., either larger molecular weight carboxylic acids or carbonyl-containing compounds – such as esters, aldehydes, and ketones. This is consistent with dimer and oligomer formation in aqueous-phase phenol SOA reactions, with the greatest proportion in samples containing syringol and guaiacol precursors (Sun et al., 2010). Small carboxylic acids, however, represent a greater percentage of phenol SOA carbonyl-containing products, at least under some conditions. This is consistent with AMS observations that the average oxygen-to-carbon ratio of SOA is highest in phenol SOA compared to guaiacol and syringol SOA (Yu et al., 2014).

The contributions of individual organic ions detected by IC – malate ($C_4H_4O_5^{2-}$), fumarate ($C_4H_2O_4^{2-}$), malonate ($CH_2(COO)_2^{2-}$), oxalate ($C_2O_4^{2-}$), maleate ($C_4H_2O_4^{2-}$), pyruvate ($C_3H_3O_3^-$), formate (CHO_2^-), and glyoxylate ($C_2HO_3^-$) – are shown in Fig. 6. In syringol and hardwood SOA samples, formate/glyoxylate and oxalate are the dominant identified acids. In guaiacol SOA samples, oxalate is the predominant ion, while malate dominates in phenol SOA and softwood SOA. The presence of these ions indicates that aqueous reactions of phenols produces some ring-opening aliphatic products, consistent with previous findings by Sun et al., 2010.

3.4. Measurement of other functional groups

Masses of saturated C–H, unsaturated C–H, and O–H in the SOA samples were determined using the calibrations reported in Fig. S4 and are reported in Table S3. We calibrated the C–H region with only compounds containing O–H, as we expected O–H to be present in all of our SOA samples. Due to blank filter variability in the O–H region and values below detection limits, we consider the O–H functional group measurement to be qualitative. Because the unsaturated C–H calibration contained only two standard compounds (both phenols), we mark this region as semi-quantitative. Saturated C–H values are quantitative with only two samples below MDL.

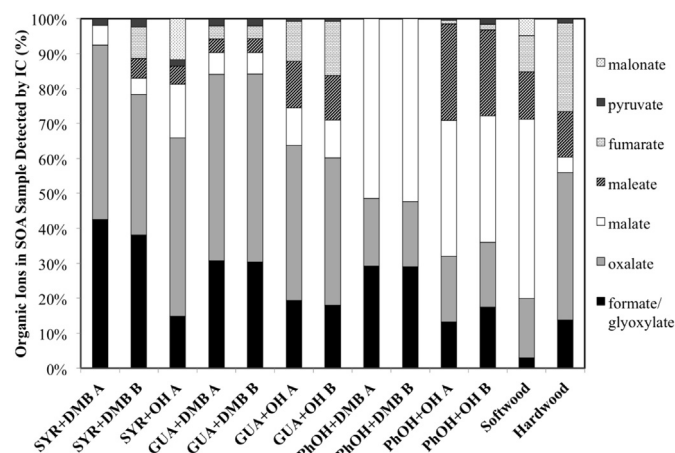


Fig. 6. A breakdown of ions detected in IC analysis of phenolic SOA samples. IC data is present for all samples except SYR + OH B.

As shown in Fig. 7, saturated C–H comprises less than 12% of total SOA sample mass with the greatest amount present in phenol samples oxidized with OH. For samples made from precursors other than phenol SOA, saturated C–H makes up an average $4 \pm 1\%$ of total SOA mass. Measurement of saturated C–H in all SOA samples confirms that some products are aliphatic in nature.

Unsaturated C–H is greatest in guaiacol SOA made with OH and in phenol SOA; it is generally lowest in syringol and hardwood SOA. The unsaturated C–H functional group has the most variability within a phenolic group, making it difficult to identify trends specific to a particular phenol. However, the presence of unsaturated C–H in all samples indicates that aromaticity is retained in the SOA. O–H functional group values are below MDL in nearly half of the samples analyzed. The greatest proportion of O–H to total SOA mass is present in phenol, softwood, and hardwood SOA samples.

Together, the four functional groups identified by FT-IR account for 24–75% (mean \pm standard deviation is $48 \pm 16\%$) of the SOA mass (Fig. 7). SOA from phenol and guaiacol via OH oxidation, and from the softwood and hardwood mixtures, had some of the highest amounts of identified mass. The disparity between gravimetric SOA mass and FT-IR identified mass suggests the samples contain additional functional groups that are not quantified by FT-IR. For example, our analysis method does not account for C–O–C bonds (which are masked by a large Teflon absorbance) and C–C bonds (which have no dipole moment). We also cannot quantify the C=C=C in aromatic rings due to spectral overlap of different functional groups in the aromatic region. Our technique therefore underestimates carbon present in aromatic rings.

3.5. Summary

In this study, we utilized FT-IR to characterize the functional groups in SOA formed via aqueous-phase photochemical reactions of phenols. Functional groups qualitatively identified include O–H, saturated C–H, unsaturated C–H, C=O, and C=C–C aromatic rings. We applied a calibration technique to the C=O, saturated C–H, unsaturated C–H and O–H functional groups to quantify these with our primary focus on carbonyl. SOA products contained a significant proportion of carbonyl-containing compounds that were formed during oxidation of the phenols. SOA from syringol contained the greatest percentage of carbonyl. Small organic acids detected by IC accounted for a small portion of the carbonyl quantified by FT-IR, indicating that most of the SOA carbonyls are

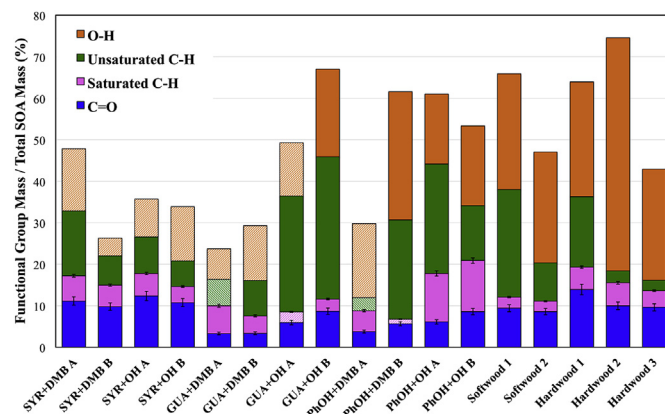


Fig. 7. Contributions of C=O, saturated C–H, unsaturated C–H and O–H to total SOA mass. Error bars for C=O and saturated C–H represent measurement uncertainty (Table S3). Values for C=O and saturated C–H are quantitative, while values for unsaturated C–H are semi-quantitative and those for O–H are qualitative. Hatching indicates values below MDL.

either in higher molecular weight carboxylic acids or in ketones, esters, aldehydes, and/or ketones. These latter carbonyl types – aldehydes and ketones – are important because they absorb solar radiation and thus might contribute to light absorption by phenolic SOA.

Acknowledgments

The authors gratefully acknowledge the National Science Foundation (Grant No. AGS-1036675) for funding.

Appendix A. Supplementary data

Supplementary data related to this article can be found at <http://dx.doi.org/10.1016/j.atmosenv.2014.11.011>.

References

- Anastasio, C., Faust, B.C., Rao, C.J., 1997. Aromatic carbonyl compounds as aqueous-phase photochemical sources of hydrogen peroxide in acidic sulfate aerosols, fogs, and clouds. 1. Non-phenolic methoxybenzaldehydes and methoxyacetophenones with reductants (phenols). *Environ. Sci. Technol.* 31 (1), 218–232.
- Chang, J.L., Thompson, J.E., 2010. Characterization of colored products formed during irradiation of aqueous solutions containing H₂O₂ and phenolic compounds. *Atmos. Environ.* 44, 541–551.
- Coates, J., 2000. Interpretation of infrared spectra, a practical approach. In: Meyers, R.A. (Ed.), *Encyclopedia of Analytical Chemistry*, pp. 10815–10837.
- Coury, C., Dillner, A.M., 2008. A method to quantify organic functional groups and inorganic compounds in ambient aerosols using attenuated total reflectance FT-IR spectroscopy and multivariate chemometric techniques. *Atmos. Environ.* 42 (23), 5923–5932.
- Donahue, N.M., Henry, K.M., Mentel, T.F., Kiendler-Scharr, A., Spindler, C., Bohn, B., Brauers, T., Dorn, H.P., Fuchs, H., Tillmann, R., Wahner, A., Saathoff, H., Naumann, K.H., Mohler, O., Leisner, T., Müller, L., Reinnig, M.C., Hoffmann, T., Salo, K., Hallquist, M., Frosch, M., Bilde, M., Tritscher, T., Barmet, P., Praplan, A.P., DeCarlo, P.F., Dommen, J., Prevot, A.S.H., Baltensperger, U., 2012. Aging of biogenic secondary organic aerosol via gas-phase OH radical reactions. *Proc. Natl. Acad. Sci. U. S. A.* 109, 13503–13508.
- Ervens, B., Turpin, B.J., Weber, R.J., 2011. Secondary organic aerosol formation in cloud droplets and aqueous particles (aqSOA): a review of laboratory, field and model studies. *Atmos. Chem. Phys.* 11, 11069–11102.
- Hallquist, M., Wenger, J.C., Baltensperger, U., Rudich, Y., Simpson, D., Claeys, M., Dommen, J., Donahue, N.M., George, C., Goldstein, A.H., Hamilton, J.F., Herrmann, H., Hoffmann, T., Iinuma, Y., Jang, M., Jenkin, M.E., Jimenez, J.L., Kiendler-Scharr, A., Maenhaut, W., McFiggans, G., Mentel, Th. F., Monod, A., Prévôt, A.S.H., Seinfeld, J.H., Surratt, J.D., Szmigielski, R., Wildt, J., 2009. The formation, properties and impact of secondary organic aerosol: current and emerging issues. *Atmos. Chem. Phys.* 9, 5155–5236.
- Hawthorne, S.B., Krieger, M.S., Miller, D.J., Mathiason, M.B., 1989. Collection and quantitation of methoxylated phenol tracers for atmospheric pollution from residential wood stoves. *Environ. Sci. Technol.* 23, 470–475.
- Heald, C.L., Kroll, J.H., Jimenez, J.L., Docherty, K.S., DeCarlo, P.F., Aiken, A.C., Chen, Q., Martin, S.T., Farmer, D.K., Artaxo, P., 2010. A simplified description of the evolution of organic aerosol composition in the atmosphere. *Geophys. Res. Lett.* 37, IMPROVE website. <http://vista.cira.colostate.edu/improve/> (July 1, 2013).
- McDade, C.E., Dillner, A.M., Indresand, H., 2009. Particulate matter sample deposit geometry and effective filter face velocities. *J. Air Waste Manag. Assoc.* 59 (9), 1045–1048.
- Najera, J.J., Percival, C.J., Horn, A.B., 2009. Infrared spectroscopic studies of the heterogeneous reaction of ozone with dry maleic and fumaric acid aerosol particles. *Phys. Chem. Chem. Phys.* 11, 9093–9103.
- Nakao, S., Clark, C., Tang, P., Sato, K., Cocker III, D., 2011. Secondary organic aerosol formation from phenolic compounds in the absence of NO_x. *Atmos. Chem. Phys.* 11, 10649–10660.
- Ofner, J., Krueger, H.U., Grothe, H., Schmitt-Kopplin, P., Whitmore, K., Zetzsch, C., 2011. Physico-chemical characterization of SOA derived from Catechol and Guaiacol—a model substance for the aromatic fraction of atmospheric HULIS. *Atmos. Chem. Phys.* 11, 1–15.
- Ofner, J., Krüger, H.U., Zetzsch, C., 2010. Time resolved infrared spectroscopy of formation and processing of secondary organic aerosols. *J. Phys. Chem.* 224, 1171–1183.
- Polidori, A., Turpin, B.J., Davidson, C.I., Rodenburg, L.A., Maimone, F., 2008. Organic PM_{2.5}: fractionation by polarity, FTIR spectroscopy, and OM/OC ratio for the Pittsburgh aerosol. *Aerosol Sci. Technol.* 42, 233–246.
- Rudich, Y., Donahue, N.M., Mentel, T.F., 2007. Aging of organic aerosol: bridging the gap between laboratory and field studies. *Annu. Rev. Phys. Chem.* 58, 321–352.
- Russell, L.M., Bahadur, R., Ziemann, P.J., 2011. Identifying organic aerosol sources by comparing functional group composition in chamber and atmospheric particles. *Proc. Natl. Acad. Sci. U. S. A.* 108 (9), 3516–3521.
- Russell, L.M., Bahadur, R., Hawkins, L.N., Allan, J., Baumgardner, D., Quinn, P.K., Bates, T.S., 2009. Organic aerosol characterization by complementary measurements of chemical bonds and molecular fragments. *Atmos. Environ.* 43 (38), 6100–6105.
- Ruthenburg, T.C., Perlin, P., Liu, V., McDade, C., Dillner, A.M., 2013. Determination of organic matter and organic carbon ratios by infrared spectroscopy with application to selected sites in the IMPROVE network. *Atmos. Environ.* 86, 47–57.
- Sander, R., 1999. In: *Compilation of Henry's Law Constants for Inorganic and Organic Species of Potential Importance in Environmental Chemistry*, third ed. Max-Planck Institute of Chemistry.
- Schauer, J.J., Kleeman, M.J., Cass, G.R., Simoneit, B.R.T., 2001. Measurement of emissions from air pollution sources. 3. C-1–C-29 organic compounds from fireplace combustion of wood. *Environ. Sci. Technol.* 35, 1716–1728.
- Smith, B., 1998. *Infrared Spectral Interpretation: a Systematic Approach*. CRC Press LLC.
- Smith, J., Sio, V., Anastasio, C., 2014. Secondary organic aerosol production from aqueous reactions of atmospheric phenols with an organic triplet excited state. *Environ. Sci. Technol.* 48 (2), 1049–1057.
- Sun, Y., Zhang, Q., Anastasio, C., Sun, J., 2010. Insights into secondary organic aerosol formed via aqueous phase reactions of phenolic compounds based on high resolution mass spectrometry. *Atmos. Chem. Phys. Discuss.* 10, 2915–2943.
- Takahama, S., Johnson, A., Russell, L., 2013a. Quantification of carboxylic and carbonyl functional groups in organic aerosol infrared spectra. *Aerosol Sci. Technol.* 47 (3).
- Takahama, S., Johnson, A., Morales, J.G., Russell, L., Duran, R., Rodriguez, G., et al., 2013b. Submicron organic aerosol in Tijuana, Mexico, from local and Southern California sources during the CalMex Campaign. *Atmos. Environ.* 70, 500–512.
- Takahama, S., Schwartz, R.E., Russell, L.M., Macdonald, A.M., Sharma, S., Leitch, W.R., 2011. Organic functional groups in aerosol particles from burning and non-burning Forest emissions at a high-elevation mountain site. *Atmos. Chem. Phys.* 11, 6367–6386.
- Yee, L.D., Kautzman, K.E., Loza, C.L., Schilling, K.A., Coggon, M.M., 2013. Secondary organic aerosol formation from biomass burning intermediates: phenol and methoxyphenols. *Atmos. Chem. Phys.* 13, 3485–3532.
- Yu, L., Smith, J., Laskin, A., Anastasio, C., Laskin, J., Zhang, Q., 2014. Chemical characterization of phenolic SOA formed from the aqueous-phase reactions with triplet excited-states of carbonyl (3C*) and hydroxyl radical (·OH). *Atmos. Chem. Phys. Discuss.* 14, 21149–21187.